

Electronic Supplementary Information

Root-like Polyamide Membranes with Fast Water Transport for Nanofiltration

Shuangqiao Han,^a Zheng Wang,^a Shenzen Cong,^a Junyong Zhu,^{*a} Xiang Zhang,^a

Yatao Zhang^{*a, b}

^a School of Chemical Engineering, Zhengzhou University, Zhengzhou 450001, PR China

E-mail: zhujunyong@zzu.edu.cn; zhangyatao@zzu.edu.cn

^b Engineering Research Center of Advanced Manufacturing of Ministry of Education, Zhengzhou

University, Zhengzhou 450001, China

Contents

1 Experimental Procedures	3
1.1 Materials	3
1.2 Preparation of ZIF-L nanoparticles with dagger-like structure	3
1.3 Preparation of polyamide membrane	4
2 Nanofiltration (NF) measurements	5
3 Calculation of membrane surface crosslinking degree	6
4 Characterization methods	6
5 Supplementary Figures	8
6 Supplementary Tables	24
7 Supplementary References.	26

1 Experimental Procedures

1.1 Materials.

Trimesoyl chloride (TMC > 98.0%), piperazine anhydrous (PIP > 99.0%), polyvinyl alcohol (PVA, Mw 85,000-124,000, 87-89% hydrolyzed), n-decane (C₁₀H₂₂ > 99.0%) were purchased from Sigma-Aldrich (St. Louis, Missouri, United States). Hydrogen chloride (HCl > 36.0%), sodium chloride (NaCl > 99.5%), sodium sulfate (Na₂SO₄ > 99.0%), magnesium sulfate (MgSO₄ > 99.5%), magnesium chloride (MgCl₂ > 99.0%), calcium chloride (CaCl₂ > 99.0%) were obtained from Sinopharm Chemical Reagent (Shanghai, China). Zn(NO₃)₂·6H₂O, 2-methylimidazole, anhydrous piperazine were purchased from Sigma-Aldrich. Polysulfone (PAN) support were kindly provided by the beginning of the science and technology limited company, (The Water flux is >500LMH, GC-UF0401, The second batch, HeNan, Zhengzhou, China).

1.2 Preparation of ZIF-L nanoparticles with dagger-like structure.

The synthesis procedure of ZIF-L nanocrystals was referenced by our previously reported.²⁹ Detailed description is as following: 2.900 g of Zn(NO₃)₂·6H₂O was dissolved in 100mL deionized water, 6.840 g 2-methylimidazole was dissolved in another 100 mL deionized water. Then the zinc nitrate/deionized aqueous solution was quickly added to the 2-methylimidazole solution and keeping stirring for 60 min at ambient temperature. The product was centrifuged at 8000 rpm for 10 minutes when the reaction finished and washed three times with deionized water. The ZIF-L obtained by drying in a vacuum oven at 40 °C for 12 hours and grinding into a

uniform powder pattern for further analysis. C, 42.18; H, 4.3; N, 24.6 %; Found (wt%): C, 41.54; H, 4.86; N, 24.39 %.

1.3 Preparation of polyamide membrane.

Hydrolysis of PAN membranes: The PAN membranes were hydrolyzed by immersion in NaOH aqueous solution (1 mol / L) at 50 °C for 1 h. Then the membranes were completely rinsed with deionized water until the pH value of the washed water reached ca. 7.0. Thus, the nitril groups of the PAN substrate were converted to the carboxylic groups that make the porous substrate more hydrophilic.

Preparation of polyamide membrane: the root-like NF membranes were prepared based-on PAN substrate membrane via optimizing the concentration of ZIF-L and PVA. The detailed prepared process can be description as following: the 10 ml of ZIF-L solution (5 mg ZIF-L nanocrystals) were dispersed with 100 ml of aqueous solution via vacuum filtration to a surface area of 8.491×10^{-3} m² PAN substrate membrane surface as a sacrificial layer template. The interfacial polymerization process was carried out on a PAN membrane with ZIF-L nanoparticles, and the aqueous solution with 10 mL of 0.194 mg/ml PIP and 0.149 mg/ml of PVA were poured into the PAN membrane for 5 min. Subsequently, the solution was poured out and the excess solution was washed off by absorbent paper. The soaked PAN membrane was dried at room temperature until there were without significant water spots on the surface of the membrane. Then, a solution of 0.212 mg/ml TMC in n-hexane was gently poured into the PAN membrane for 1 minute. The prepared PA membrane was immediately dried in an oven at a temperature of 80 °C for 10

min. The root-like structure PA membrane was prepared via etching away the ZIF-L nanoparticles of the PA membrane in hydrochloric acid solution. The membrane was washed three times with deionized water before use.

2 Nanofiltration (NF) measurements

In this work, the performance of the membranes were tested via using a cross-flow NF unit with a separation area of 7.1 cm² at room temperature. The membrane was pre-pressed for one hour and regulated operating pressures from 0.2 to 0.8 MPa prior to each experiment. The pure water permeability and water flux of the membrane were tested at 0.4 MPa. The pumping system is measured at a constant pressure and the water flux is calculated according to equation (1):

$$J = \frac{V}{A\Delta t} \quad (1)$$

Where J is the flux of the membranes, V is volume increase of permeate during filtration time Δt , A is the effective area of the tested membrane.

Here, the permeability (P) is defined as the flow rate per unit of applied pressure, calculated by the formula (2), where ΔP is the transmembrane pressure of the filtration experiment.

$$P = \frac{J}{\Delta P} \quad (2)$$

When measuring the rejection of the membrane, the deionized water is replaced with the feed solution, which is pumped into the system at a constant pressure of 0.4 MPa. The waste liquid is calculated from the conductivity of the feed and the

filtrate by the formula (3), where C_f and C_p represent the conductivity of the feed solution and the waste liquid, respectively.

$$R = 1 - \frac{C_p}{C_f} \quad (3)$$

In order to check the accuracy and reproducibility of the results, three filtration experiments were performed on three different membranes with same concentrations of solution, and the average of the pure water flux and rejection of the membrane surface was calculated.

3 Calculation of membrane surface crosslinking degree

According to the O/N element ratio of XPS spectrum, the degree of crosslinking of the PA active layer was calculated. The O/N ratio can be calculated by equation (4), where A and B represent the fully cross-linked portion and the linear cross-linked portion, respectively. The cross-link density (C) can be calculated by formula (5).

$$\frac{O}{N} = \frac{3A + 4B}{3A + 2B} \quad (4)$$

$$C = \frac{A}{A + B} \quad (5)$$

4 Characterization methods

Surface physicochemical properties (e.g., elemental composition, thermostability, hydrophilicity, structure and surface charge) and morphology were determined by X-ray photoelectron spectroscopy (XPS), X-ray diffractometer (XRD), atomic force

microscopy (AFM), scanning electron microscopy (SEM), thermogravimetric analysis (TGA), Attenuated total reflection Fourier transform infrared (ATR-FTIR), contact angle (CA) and zeta potential, respectively. XRD analysis of membranes was carried out on a PANalytical X'Pert Pro (PANalytical, The Netherlands) in the scanning range of 2θ between 10° and 60° using copper $K\alpha$ as the source of radiation, and a step size of 0.02° . XPS (K-alpha, Thermo Fisher, USA) was used to analyze the surface chemical functionality. The cross-sectional morphologies and membrane surface were examined with scanning electron microscopy (SEM, JSM-6700F, JEOL, and Japan) operating at 10.0 kV. The TGA was carried out using NETZSCH TG 209 (Germany) instrument under a nitrogen atmosphere with a heating rate of $10^\circ\text{C}/\text{min}$ from room temperature to 650°C . The surface morphologies and roughness were obtained by AFM (Bruker Dimension Fastscan, USA) at the ScanAsyst mode. The water contact angles (WCA) of the membranes were measured by a contact angle goniometer (Maist Drop Meter A-100P) equipped with a highspeed charge-coupled device (CCD) camera via the sessile drop method. The ZP values of the membranes were recorded through a SurPASS™ 3 electrokinetic analyzer (Anton Paar, Graz, Austria) with an adjustable gap cell. The ZP values were determined in a background electrolyte of 1 mM KCl solution over a pH range from 3 to 10 at room temperature. ATR-FTIR spectroscopy ($4000\text{-}400\text{ /cm}$) was collected on a FT-IR spectrometer in the membranes state.

5 Supplementary figures

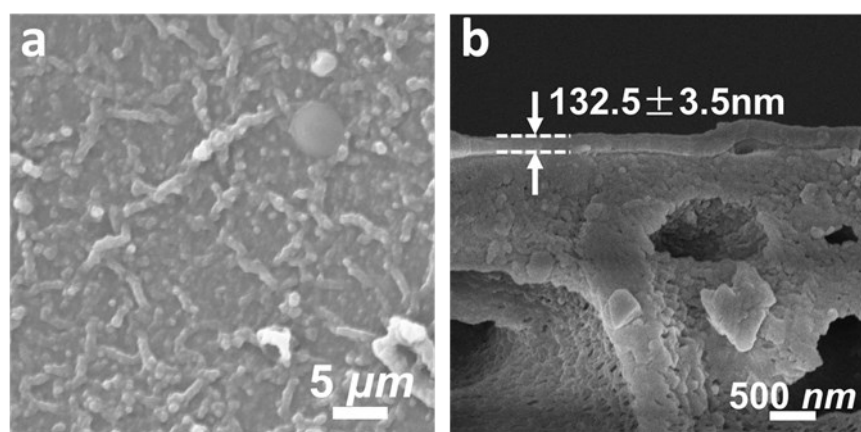


Fig. S1 SEM images of PPA membrane (a) surface and (b) cross-section.

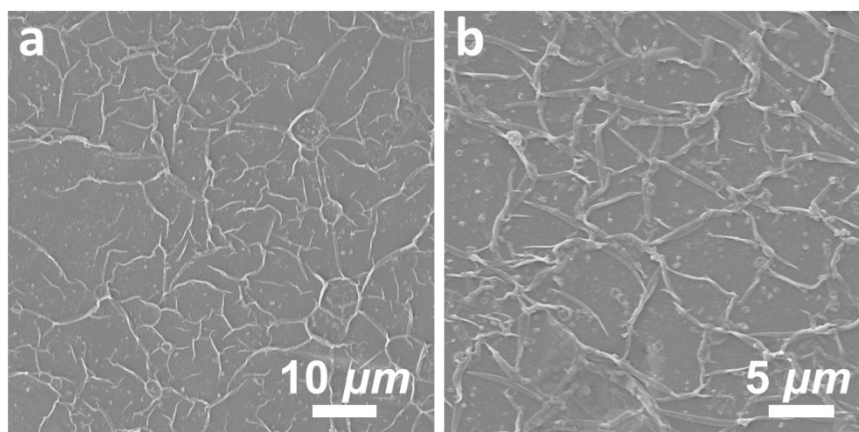


Fig. S2 Surface SEM images of P-PPA membrane (a) scale: 10 μ m and (b) scale: 5 μ m.

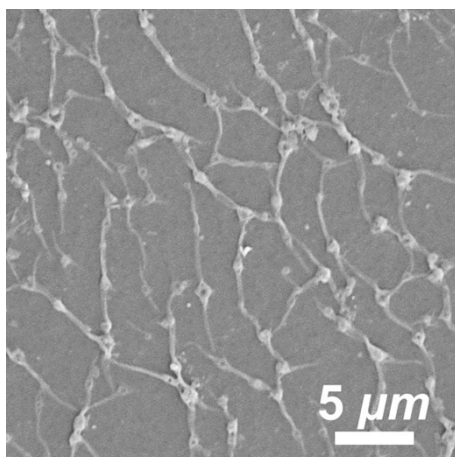


Fig. S3 Surface SEM images of Z-PPA membrane (scale:5μm).

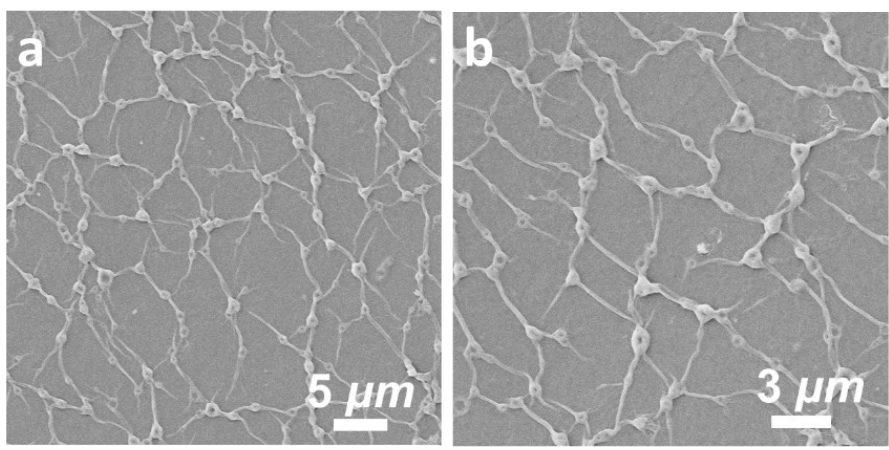


Fig. S4 Surface SEM images of E-PPA membrane (a) scale: 5μm and (b) scale: 3μm.

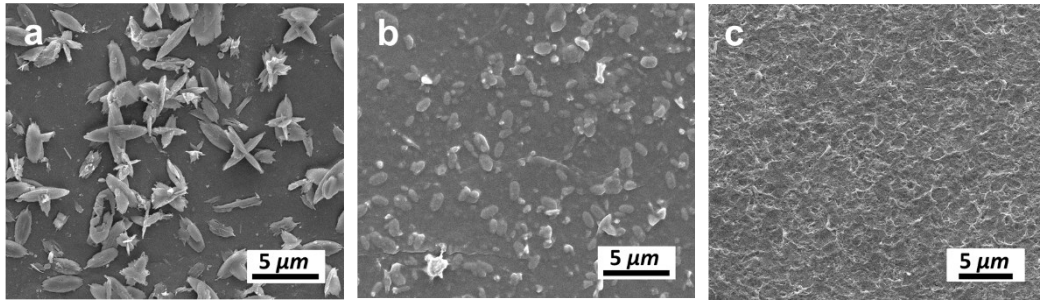


Fig. S5 (a) Surface SEM image of 0.005 wt% nanoparticles supported on PAN membrane. (b) Surface SEM image of the as-prepared membrane after an IP process without PVA. (c) Surface SEM image of the as-prepared membrane after acid treatment without PVA.

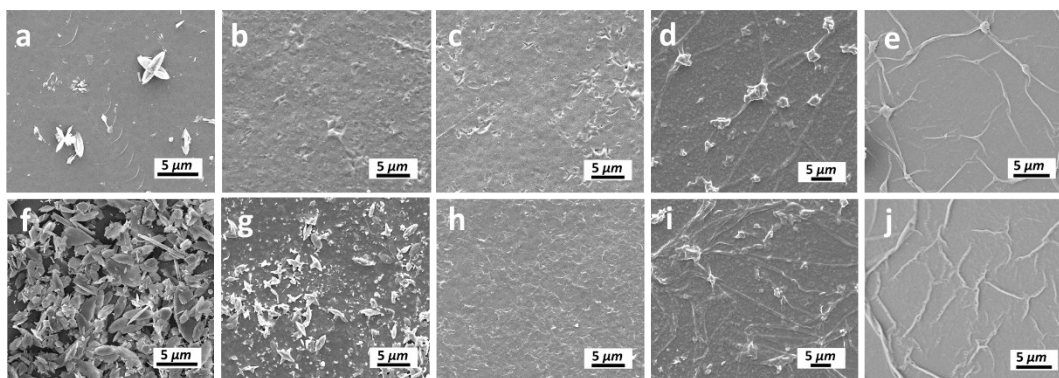


Fig. S6 Surface SEM images of the membranes with underlying loaded nanoparticles (a) 0.0025 wt%, (f) 0.0075 wt%. Surface SEM images of the membranes after IP process without PVA (b) 0.0025 wt%, (g) 0.0075 wt%. Surface SEM images of the membranes after After acid treatment without PVA (c) 0.0025 wt%, (h) 0.0075 wt%. Surface SEM images of the membranes after IP process with PVA (d) 0.0025 wt%, (i) 0.0075 wt%. Surface SEM images of the membranes after After acid treatment with PVA (e) 0.0025 wt%, (j) 0.0075 wt%.

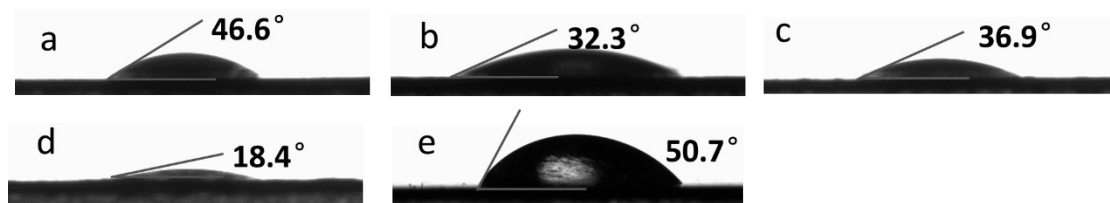


Fig. S7 contact angle of the prepared membranes: (a) PPA membrane, (b) P-PPA membrane, (c)Z-PPA membrane, (d) E-PPA membrane and (e) 0.075 wt% ZIF-L-loaded membrane.

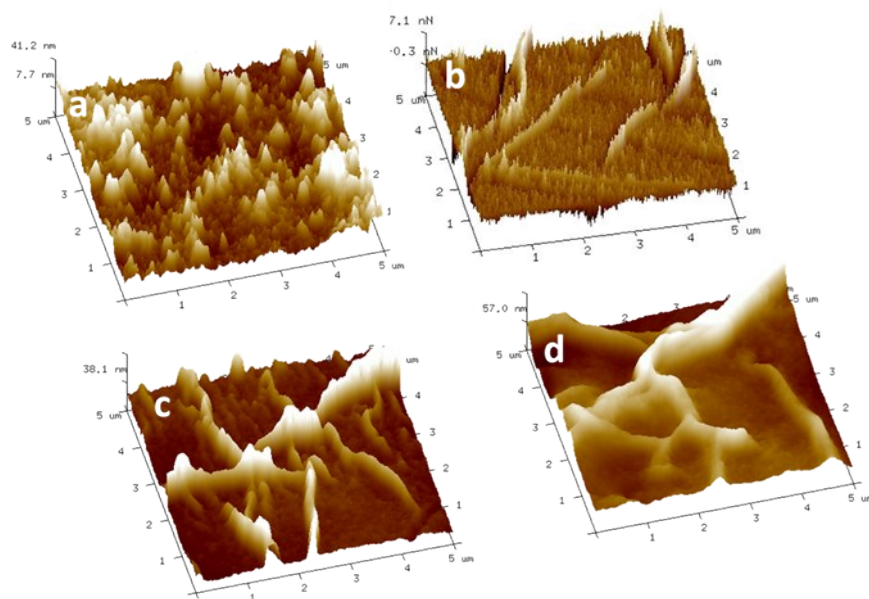


Fig. S8 AFM images of all the PA membranes fabricated in this study: (a) PPA membrane, (b) P-PPA membrane, (c) Z-PPA membrane and (d) E-PPA membrane.

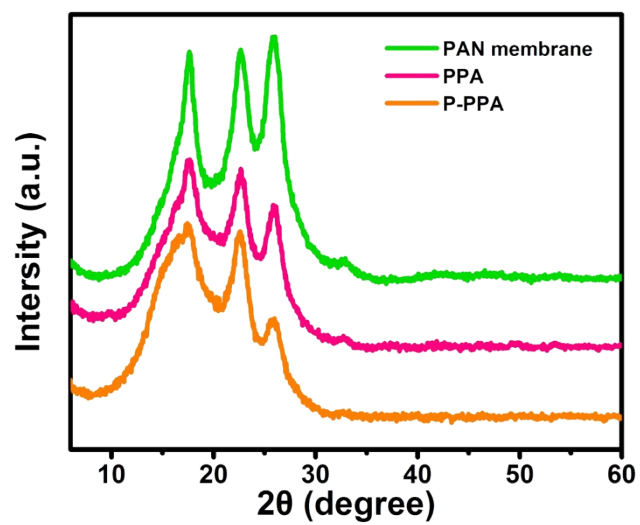


Fig. S9 XRD patterns of pristine PAN membrane, PPA membrane and P-PPA membrane.

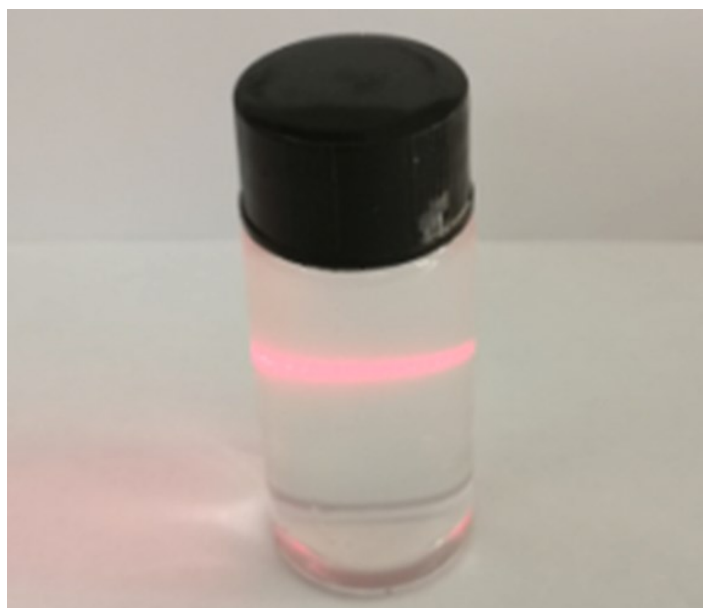


Fig. S10 Photo images of aqueous suspension containing ZIF-L nanoparticles after 24 h standing.

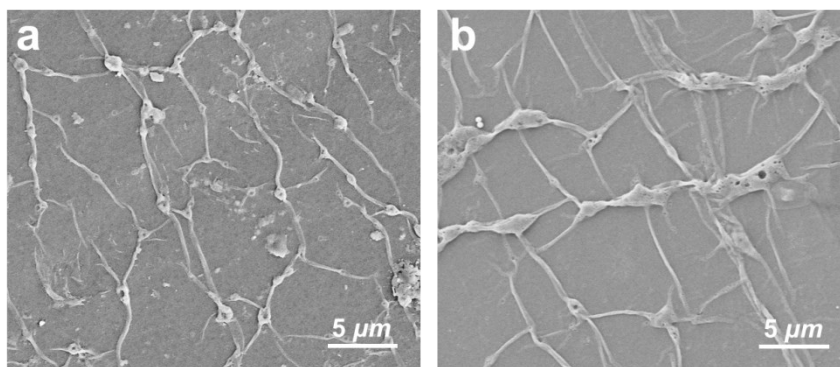


Fig. S11 Surface SEM images of the Z-PPA membrane adding in acid solution: (a) 12 hours and (b) 24 hours.

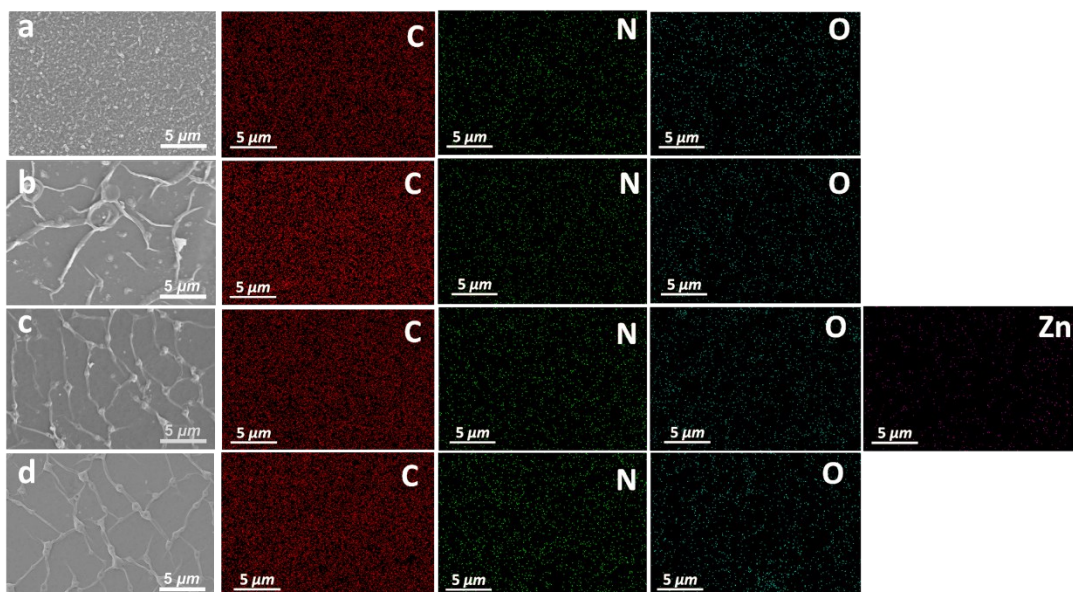


Fig. S12 Zinc distribution map, Carbon distribution map, Nitrogen distribution map, Oxygen distribution map of the resulting membranes (a) PPA membrane, (b) p-PPA membrane, (c) Z-PPA membrane and (d) E-PPA membrane.

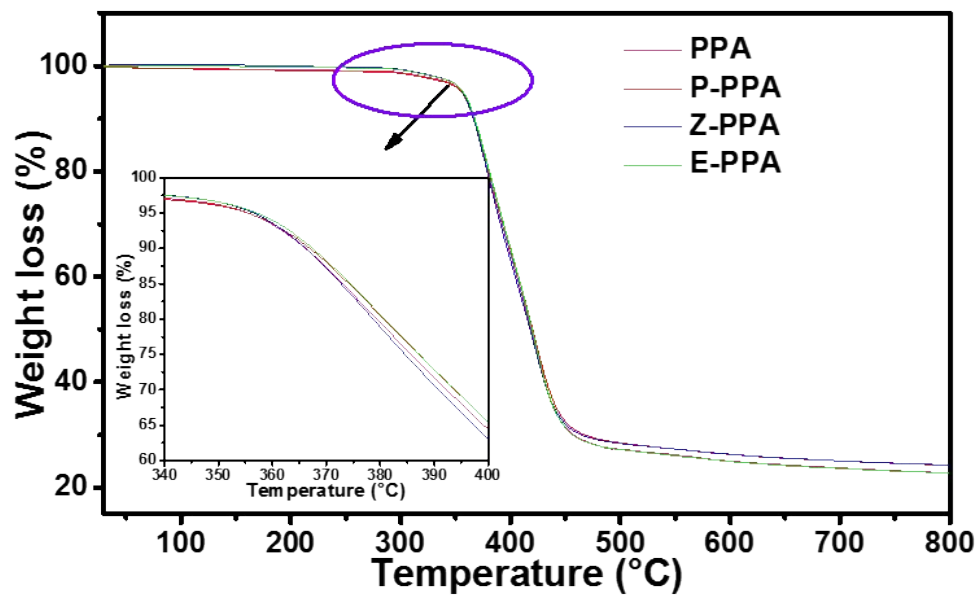


Fig. S13 The thermogravimetric curve of the prepared membranes.

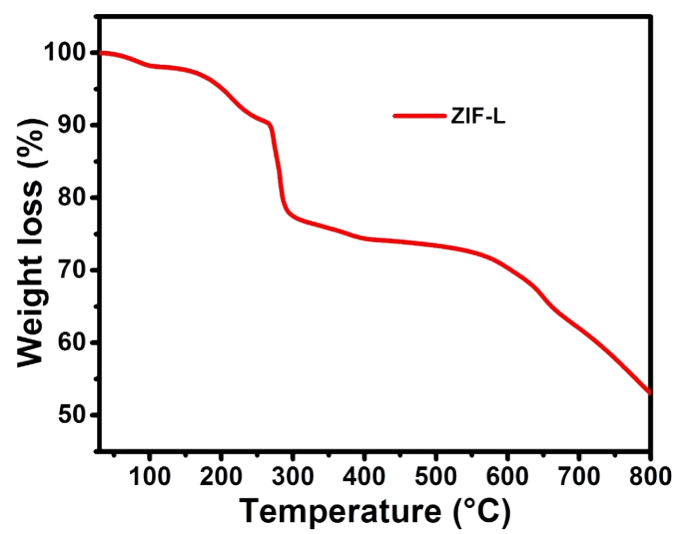


Fig. S14 Thermogravimetric analysis (TGA) on ZIF-L under N₂ atmosphere.

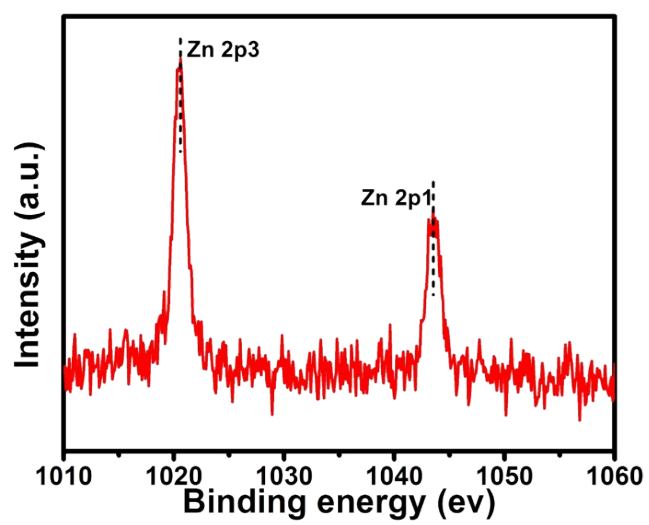


Fig. S15 Zn 2p core-level spectra of Z-PPA membrane.

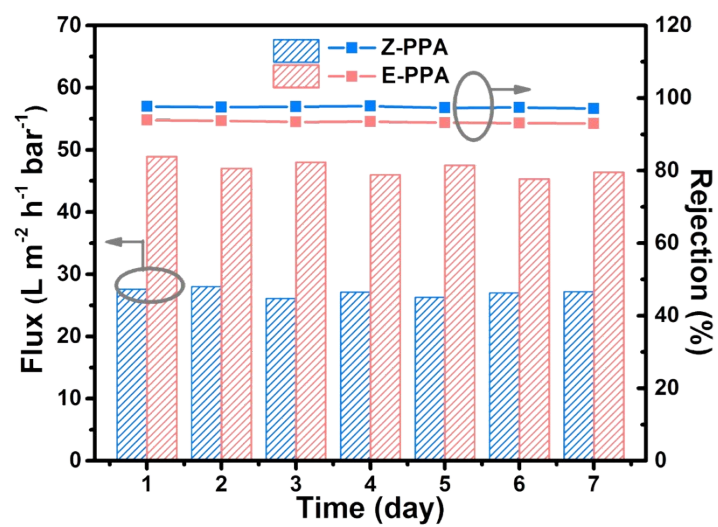


Fig. S16 Stability of Z-PPA and E-PPA membranes under long-term nanofiltration operation.

6 Supplementary Tables

Table S1: Height, root average arithmetic roughness (Ra) and root mean surface roughness (Rq) values of prepared membranes.

Samples	Height (nm)	Image Rq (nm)	Image Ra (nm)
PPA	41.2	10.2	7.4
P-PPA	134.4	24.8	16.4
Z-PPA	132.2	29.8	22.6
E-PPA	373.3	77.9	60.2

Table S2: The atomic concentrations of different elements in the membrane and the crosslinking degree of the prepared membrane.

Samples	Atomic concentrations (%) of different elements				Crosslinking degree (%)
	C	N	O	Zn	
PPA	73.81	11.80	14.39	-	70.2
P-PPA	76.45	10.49	13.07	-	66.7
Z-PPA	70.22	11.71	17.65	0.41	40.0
E-PPA	73.32	10.33	16.15	-	33.9

Table S3: The Surface chemical species from C1s.

Samples	Surface chemical species from C1s		
	B.E. (eV)	Species	Content (%)
PPA	284.8	C-H/C-C	58.62
	286.0	C-N	34.64
	288.0	O-C=O/O-C=N	6.75
P-PPA	284.8	C-H/C-C	59.86
	286.0	C-N	26.65
	288.0	O-C=O/O-C=N	13.49
Z-PPA	284.8	C-H/C-C	60.60
	286.0	C-N	26.42
	288.0	O-C=O/O-C=N	12.97
E-PPA	284.8	C-H/C-C	60.04
	286.0	C-N	27.04
	288.0	O-C=O/O-C=N	12.68

References

1. G. Gong, P. Wang, Z. Zhou and Y. Hu, *ACS Appl. Mater. Interfaces*, 2019, **11**, 7349-7356.
2. F. Y. Zhao, Y. L. Ji, X. D. Weng, Y. F. Mi, C. C. Ye, Q. F. An and C. J. Gao, *ACS Appl. Mater. Interfaces*, 2016, **8**, 6693-6700.
3. J. Zhu, W. Hou, J. Zhang, S. Yuan, J. Li, M. Tian, H. Wang, T. Zhang, A. Volodind and B. Van der Bruggen, *J. Mater. Chem. A*, 2018, **6**, 15701-15709.
4. H. Wang, L. Chen, H. Yang, M. Wang, L. Yang, H. Du, C. Cao, Y. Ren, Y. Wu, F. Pan and Z. Jiang, *J. Mater. Chem. A*, 2019, **7**, 20317-20324.
5. X. Song, B. Gan, Z. Yang, C. Y. Tang and C. Gao, *J. Membr. Sci.*, 2019, **582**, 342.
6. H. B. Park, J. Kamcev, L. M. Robeson, M. Elimelech and B. D. Freeman, *Science*, 2017, **356**, eaab0530.